# Tuning an Activator-Repressor Clock Employing Retroactivity

Alexander Rosenberg*, Shridhar Jayanthi† and Domitilla Del Vecchio‡
*Electrical Engineering Dept., University of Washington, Seattle WA 98195
†Electrical Engineering and Computer Science Dept., University of Michigan, Ann Arbor MI 48109
‡Dept. of Mechanical Engineering, Massachusetts Institute of Technology, Cambridge MA 02139

***Abstract*— Activator-repressor systems have been shown to be capable of oscillations and are therefore an important clock motif in the field of Synthetic and Systems Biology. In this paper, we propose a method to regulate oscillatory behavior in such systems by the addition of DNA binding sites for the proteins involved in the clock network. We show that the retroactivity effect caused by this addition can effectively change the relative timescales among the protein dynamics and impact the behavior of the clock. We also employ root locus analysis to obtain a graphical interpretation of the results.**

## I. Introduction

The design and analysis of oscillating modules is important in the fields of Systems and Synthetic Biology as it enables the understanding of oscillator mechanisms that regulate essential natural processes, such as the cell cycle [1] or circadian clocks [2]. Oscillators are also a useful module in Synthetic Biology as they allow for synchronization of different modules leading to more complex design [3]. Several synthetic oscillators have been proposed and implemented [4]–[7]. In this paper, we analyze one such module, the *activator-repressor clock* of [6]. This oscillator is composed by two proteins, an *activator protein* A that promotes the expression of itself and of a *repressor protein* R. The repressor protein, in turn, represses the expression of the activator protein providing a negative feedback loop. This system is illustrated in Figure 1(a).

Conditions that guarantee stable oscillations for this clock were studied in [8]. In particular, the difference of timescales between repressor and activator dynamics is shown to be a key parameter in this process. More specifically, it was shown that, by increasing the timescale of the activator with respect to that of the repressor, the system goes through a supercritical Hopf bifurcation from which a periodic orbit emerges. Altering these timescales usually involve changing the degradation and expression rates, which can be a challenge. The expression rates are usually tuned by altering promoter and ribosome binding sites [9], and degradation rates can be tuned by employing degradation tags [10].

As an alternative, we propose to change the effective relative timescales by exploiting *retroactivity* [11]. Retroactivity is the phenomenon by which a downstream system applies a load to an upstream system upon interconnection and, thus, changes its behavior. It was shown in [12] that the dynamics of transcriptional components are slowed down when the output protein is used to regulate the expression of another protein due to the interaction of the protein with DNA binding sites. This change in timescale due to retroactivity can, in principle, be employed to tune the timescales of an activator-repressor motif. This mechanism is of interest since it only requires the addition of binding sites with an affinity to either the activator protein or the repressor protein, which can be achieved through transformation of plasmids containing the specific DNA sequence. This experimental procedure is much simpler in than the alternative techniques considered above with protocols found in standard molecular biology manuals such as [13].

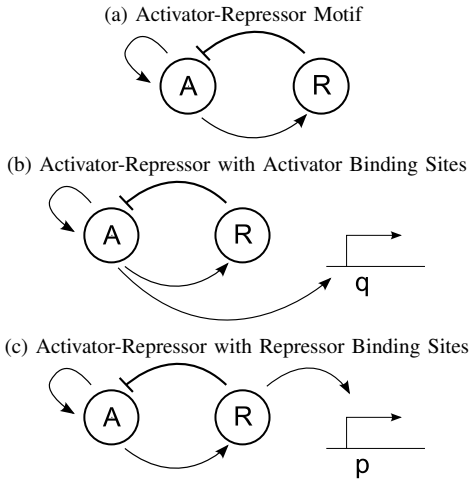


Fig. 1. Diagram (a) illustrates the activator-repressor motif. Diagram (b) and (c) illustrate the systems after the addition of DNA binding sites with affinity to the activator and the repressor respectively.

In this paper, we analyze the retroactivity effect resulting from adding binding sites to an activator-repressor clock. We show that this mechanism can be employed to silence an oscillating activator-repressor system as well as to obtain stable oscillations from an originally non-oscillating system. In particular, we consider the addition of DNA binding sites with affinity to the activator (Figure 1(b)) or to the repressor (Figure 1(c)) and show that the systems go through a Hopf bifurcation having the amount of binding sites as the bifurcation parameter.

This paper is organized as follows. In Section II, the activator-repressor clock is introduced and conditions for having oscillations are given. In Section III, the effect of the addition of DNA binding sites with affinity to the activator or to the repressor are studied. Section IV provides a graphical

interpretation of the results shown in this paper using the root locus method.

## II. Activator-Repressor Oscillator

Consider the two-component oscillator designed using the activator-repressor system of [8], illustrated in Figure 1(a). Activator protein A promotes the expression of repressor protein R which in turn represses expression of protein A. Protein A also promotes expression of itself. We consider here a one-step model for protein expression from the DNA. This is model can be obtained by employing singular perturbation to the two-step model including mRNA dynamics, as shown in [8]. The model for activator-repressor motif is given by

$$\begin{aligned} \dot{A} &= -\delta_A A + f_1(A,R) \\ \dot{R} &= -\delta_R R + f_2(A), \end{aligned} \tag{1}$$

in which $f_1(A,R)$ and $f_2(A)$ are Hill functions associated with expressions of $A$ and $R$. These functions are given by

$$f_1(A,R) = \frac{K_1 A^n + K_A}{1+\gamma_1 A^n + \gamma_2 R^n} \text{ and } f_2(A) = \frac{K_2 A^n + K_R}{1+\gamma_3 A^n},$$

in which $K_1$ and $K_2$ are the maximal expression rates when the activator protein is in excess, $K_A$ and $K_R$ are the expressions in the absence of activator or repressor, $\gamma_1$, $\gamma_2$ and $\gamma_3$ are coefficients related to the affinity between the proteins and the promoter regions, and $n$ is the Hill coefficient.

We seek structural properties for which this system presents oscillations. To this end, assume that system (1) has a single equilibrium point at $(A^*, R^*)$. Conditions for having a unique equilibrium point can be found in [8]. The Jacobian of system (1) calculated at the equilibrium is given by

$$J_0 = \begin{bmatrix} -\delta_A + \dfrac{\partial f_1(A^*,R^*)}{\partial A} & \dfrac{\partial f_1(A^*,R^*)}{\partial R} \\ \dfrac{\partial f_2(A^*)}{\partial A} & -\delta_R \end{bmatrix}. \tag{2}$$

Additionally, we assume $\det(J_0) > 0$ and $\mathrm{trace}(J_0) > 0$ so that the equilibrium point is an unstable node or spiral. This is guaranteed by the following conditions

*(i)* $\delta_A - \dfrac{\partial f_1(A^*,R^*)}{\partial A} > \dfrac{1}{\delta_R}\dfrac{\partial f_1(A^*,R^*)}{\partial R}\dfrac{\partial f_2(A^*)}{\partial A}$;

*(ii)* $\delta_A + \delta_R < \dfrac{\partial f_1(A^*,R^*)}{\partial A}$.

We seek to show that a system satisfying *(i)* and *(ii)* presents a stable periodic orbit. In order to do so, it is necessary to first show the following proposition.

*Proposition 1:* There exists a constant $D \in \mathbb{R}_+$ such that the set $K = \{(A,R) \in \mathbb{R}^2_+ | A^2 + R^2 \leq D^2\}$ is a positively invariant set under the vector field defined by system (1) and $(A^*, R^*) \in K$.

*Proof:* From the definition of the Hill functions it is clear that $f_1(A,R)$ and $f_2(A)$ are positive bounded functions. Let $M_1 = \sup\{f_1(A,R)\}$ and $M_2 = \sup\{f_2(A)\}$. We first notice that for $A = 0$, $\dot{A} > 0$ according to (1).

(a) Conditions *(i)* and *(ii)* satisfied

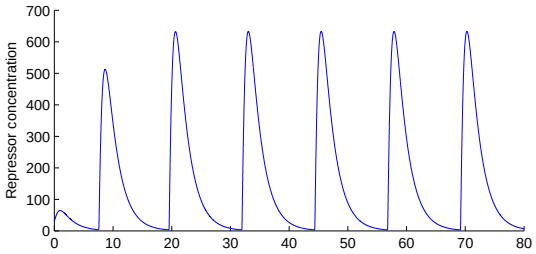


(b) Conditions *(i)* and *(ii)'* satisfied

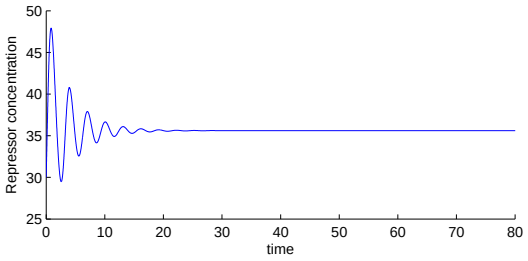


Fig. 2. These figures illustrate the effect of conditions *(ii)* and *(ii)'* in system (1). The top plot presents a simulation of system (5) while the bottom plot presents a simulation of system (10). The parameters used in this simulation are $n = 2$, $\delta_A = 1$, $k_{on} = 10$, $k_{off} = 1000$, $\gamma_1 = \gamma_2 = \gamma_3 = .1$, $K_1 = K_2 = 300$, $K_{A0} = 0.04$ and $K_{B0} = 0.004$. In the top plot $\delta_R = .5$ whereas in the bottom plot $\delta_R = 1.5$.

Similarly, for $R = 0$, $\dot{R} > 0$. The quadrant $\mathbb{R}^2_+$ is, therefore, a positively invariant set. Define $\delta^* = \min\{\delta_A, \delta_R\}$ and $M = \max\{M_1, M_2\}$. Consider the positive definite function $v(A,R) = A^2/2 + R^2/2$. Using the chain rule, it is possible to show that

$$\begin{aligned} \frac{dv(A,R)}{dt} &= -\delta_A A^2 - \delta_R R^2 + A f_1(A,R) + R f_2(R) \\ &\leq -\delta^* A^2 - \delta^* R^2 + A M_1 + R M_2 \\ &= -\delta^* \left(A - \frac{M}{2\delta^*}\right)^2 - \delta^* \left(R - \frac{M}{2\delta^*}\right)^2 + \frac{M^2}{2\delta^*}. \end{aligned}$$

From the above, it is clear that $\dot{v}(A,R) < 0$ on the exterior of a circle with center $(M/2\delta^*, M/2\delta^*)$ and radius $M/\sqrt{2}\delta^*$. Therefore, for any

$$D > \max\{\sqrt{2}M/\delta^*, A^*, R^*\},$$

we can show that $\dot{v}(A,R) < 0$ along the arc defined by the boundary of $K$. Since $v(A,R)$ is positive definite, $K$ is a positively invariant set. Also, the above choice for $D$ guarantees the equilibrium is in the interior of $K$. ■

With this Proposition, it is possible to show the following lemma.

*Lemma 1:* Consider system (1) with a single equilibrium point $(A^*, R^*)$, and let $K$ be the invariant set from Proposition 1. Assume further that the system satisfies condition *(i)* and *(ii)*. Then, for any initial condition $(A_0, R_0) \in K - \{(A^*, R^*)\}$, the $\omega$-limit set is a periodic orbit.

*Proof:* Consider the Jacobian (2) of (1), evaluated at $(A^*, R^*)$. Condition *(i)* guarantees that $\det(J_0) > 0$ and condition *(ii)* guarantees that $\mathrm{trace}(J_0) > 0$. This implies

that the real part of the eigenvalues of $J_0$ are positive and, therefore, the equilibrium point is unstable and not a saddle. Therefore, the trajectory starting at $(A_0, R_0)$, has no fixed points. It follows from the Poincar-Bendixson theorem that the $\omega$-limit set of $(A_0, R_0)$ is a periodic orbit. ■

We also consider the case in which the equilibrium of (1) is stable. It will also be useful to consider the condition under which the trace of (2) is negative:

*(ii)'* $\delta_A < \dfrac{\partial f_1(A^*, R^*)}{\partial A} < \delta_A + \delta_R.$

The first inequality in the above condition is an additional requirement that, while not essential for the stability of the equilibrium, allows tuning the system through retroactivity. The following lemma shows that this condition leads to stability of the equilibrium.

*Lemma 2:* Consider system (1) with a single equilibrium point. Assume further that the system satisfies condition *(i)* and *(ii)'*. Then, the equilibrium $(A^*, R^*)$ is asymptotically stable.

*Proof:* Consider again the Jacobian (2). Condition (i) guarantees that $\det(J_0) > 0$, while condition *(ii)'* guarantees that $\mathrm{trace}(J_0) < 0$. The real parts of the eigenvalues of the Jacobian are, thus, negative, leading to the desired result. ■

Simulation results of system (1) shown in Figure 2 illustrate the results from the Lemmas. In both simulations, the parameters were chosen so that the system satisfies conditions *(i)* as well as the uniqueness of the equilibrium point. In Figure 2(a), the system satisfies condition *(ii)* and therefore presents oscillatory behavior, whereas in Figure 2(b), condition *(ii)'* is satisfied, resulting in a system that converges to its stable equilibrium point.

## III. Addition of DNA binding sites

In this section, we consider the addition of extra DNA binding sites with affinity to the activator or repressor protein as illustrated in Figures 1(b) and 1(c), respectively. Let $q$ represent the binding sites with affinity to the activator, and $p$ represent the binding sites with affinity to the repressor. The interaction between protein and binding sites is modeled by the following reactions

$$A + q \underset{k_{u1}}{\overset{k_{b1}}{\rightleftharpoons}} C_1 \tag{3}$$

$$R + p \underset{k_{u2}}{\overset{k_{b2}}{\rightleftharpoons}} C_2, \tag{4}$$

in which $C_1$ represents the complex formed by $A$ and $q$, $C_2$ represents the complex formed by $R$ and $p$, $k_{u1}$, $k_{u2}$, $k_{b1}$, $k_{b2}$ are the dissociation and association constants between the proteins and their respective binding sites. These constants are considered to be much faster than the protein expression and degradation processes [14], and singular perturbation is employed for model reduction. We also assume the total concentration of binding sites $q_T = q + C_1$ and $p_T = p + C_2$ to be constants.

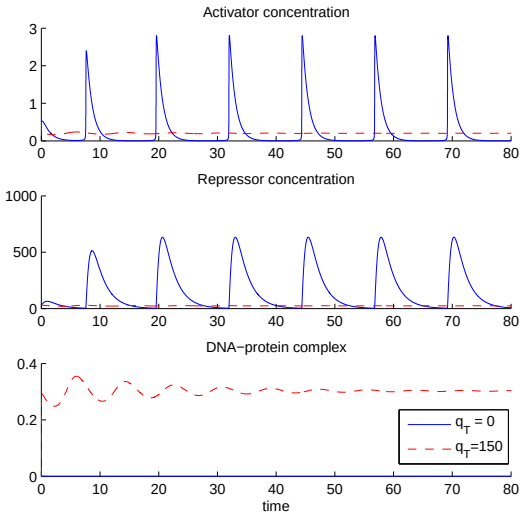


Fig. 3. These figures illustrate the stabilization of the equilibrium point resulting from the addition of DNA binding sites with affinity to the activator to an oscillating activator-repressor clock. The system presents a periodic solution when isolated ($q_T = 0$). With addition of DNA binding sites ($q_T = 150$), the solution goes to the equilibrium. System (5) was simulated with parameters $n = 2$, $\delta_A = 1$, $k_{on} = 10$, $k_{off} = 1000$, $\gamma_1 = \gamma_2 = \gamma_3 = .1$, $K_1 = K_2 = 300$, $K_{A0} = 0.04$, $K_{B0} = 0.004$ and $\delta_R = .5$.

### A. Activator Binding Sites

In this situation, we consider the system shown in Figure 1(b). To system (1), we incorporate the dynamics related to the chemical equation (3) obtaining the model

$$\begin{aligned} \dot{A} &= -\delta_A A + f_1(A, R) + k_{u1} C_1 - k_{b1} A(q_T - C_1) \\ \dot{R} &= -\delta_R R + f_2(A) \\ \dot{C}_1 &= -k_{u1} C_1 + k_{b1} A(q_T - C_1). \end{aligned} \tag{5}$$

Note that the number and location of equilibria of system (5) is the same as that of system (1).

This model is further simplified by employing a singular perturbation argument exploiting the difference of timescales. To make the timescale separation between the expression/degradation of proteins and the repressor/protein interactions explicit, define the small parameter $\epsilon := \delta_R / k_{u1}$. Define also $k_{d1} := k_{u1}/k_{b1}$ to be the dissociation constant for this interaction. Define the variable $Y_1 := A + C_1$. System (5) can be rewritten in the standard singular perturbation form [15] as

$$\begin{aligned} \dot{Y}_1 &= -\delta_A (Y_1 - C_1) + f_1(Y_1 - C_1, R) \\ \dot{R} &= -\delta_R R + f_2(Y_1 - C_1) \\ \epsilon \dot{C}_1 &= -\delta_R C_1 + \frac{\delta_R}{k_{d1}} (Y_1 - C_1)(q_T - C_1). \end{aligned}$$

Let $C_1 = \gamma(Y_1)$ be the unique solution of

$$g(C_1, Y_1) := -\delta_R C_1 + \frac{\delta_R}{k_{d1}} (Y_1 - C_1)(q_T - C_1) = 0 \tag{6}$$

under the restriction $C_1 < q_T$. One can show that

$$\left.\frac{\partial g(C, Y_1)}{\partial C}\right|_{C=\gamma(Y_1)} < 0$$

and, thus, that the slow manifold $C_1 = \gamma(Y_1)$ is attractive [11]. The reduced system is thus given by

$$\begin{aligned}\dot{A} &= [-\delta_A A + f_1(A, R)]\left(1 - \frac{\partial \gamma(Y_1)}{\partial Y_1}\right)\\ \dot{R} &= -\delta_R R + f_2(A).\end{aligned}$$

Using the implicit function theorem in the manifold equation (6), it is possible to show that

$$\frac{\partial \gamma(Y_1)}{\partial Y_1} = \frac{1}{1 + \frac{k_{d1}}{q_T}\left(1 + \frac{A}{k_{d1}}\right)^2}.$$

For compactness of notation, define the function

$$\mathcal{S}_A(A, q_T) := 1 - \frac{\partial \gamma(Y_1)}{\partial Y_1} = \frac{1}{1 + k_{d1} q_T (k_{d1} + A)^{-2}}$$

to obtain the system

$$\begin{aligned}\dot{A} &= \mathcal{S}_A(A, q_T)\,[-\delta_A A + f_1(A, R)]\\ \dot{R} &= -\delta_R R + f_2(A),\end{aligned} \tag{7}$$

a two-state system with parameter $q_T$. Note that since $\mathcal{S}_A(A, q_T) \neq 0$, the unique equilibrium of system (7) is the same as of (1), namely $(A^*, R^*)$. Furthermore, the Jacobian of system (7) is given by

$$J_A(q_T) = \begin{bmatrix} \mathcal{S}_A^*\left(-\delta_a + \frac{\partial f_1(A^*, R^*)}{\partial A}\right) & \mathcal{S}_A^* \frac{\partial f_1(A^*, R^*)}{\partial R} \\ \frac{\partial f_2(A^*)}{\partial A} & -\delta_R \end{bmatrix}, \tag{8}$$

in which we use the shorthand notation $\mathcal{S}_A^* := \mathcal{S}_A(A^*, q_T)$. Note that $0 < \mathcal{S}_A^* \leq 1$ is a strictly monotonically decreasing function of the parameter $q_T$. Note also that

$$\mathcal{S}_A^*|_{q_T=0} = 1 \text{ and } \lim_{q_T \to \infty} \mathcal{S}_A^* = 0. \tag{9}$$

The following lemma shows that an oscillating activator-repressor clock can be stabilized to the equilibrium by addition of sufficient DNA binding sites with affinity to the activator.

*Lemma 3:* Consider system (7) and let conditions *(i)* and *(ii)* be satisfied. There exists $q^* > 0$ such that the equilibrium $(A^*, R^*)$ is asymptotically stable if and only if $q_T > q^*$.

*Proof:* We first show that $\det(J_A(q_T)) > 0$ for all $q_T$. This follows from the fact that $\det(J_A(q_T)) = \mathcal{S}_A^* \det(J_0) > 0$, from condition *(i)*. We now focus on

$$\operatorname{trace}(J_A(q_T)) = \mathcal{S}_A^*\left(-\delta_a + \frac{\partial f_1(A^*, R^*)}{\partial A}\right) - \delta_R.$$

From (9) and condition *(ii)*, when $q_T = 0$ $\operatorname{trace}(J_A(0)) > 0$. Additionally, as $q_T \to \infty$, $\operatorname{trace}(J_A(q_T)) \to -\delta_R < 0$. Since the trace is a monotonic smooth function of $q_T$, one can apply the intermediate value theorem to show that there is an unique $0 < q^* < \infty$ such that $\operatorname{trace}(J_A(q^*)) = 0$. Since $\det(J_A(q^*)) > 0$, the eigenvalues of $J_A(q^*)$ are imaginary. From the monotonicity of the trace with respect to $q_T$, it follows that the real parts of the eigenvalues of $J_A(q_T)$ are positive for all $0 \leq q_T < q^*$ and negative for all $q_T > q^*$. It follows that the system goes through a Hopf bifurcation at $q_T = q^*$, and thus presents a periodic solution for $0 \leq q_T < q^*$ while it converges to the equilibrium for $q_T > q^*$. ■

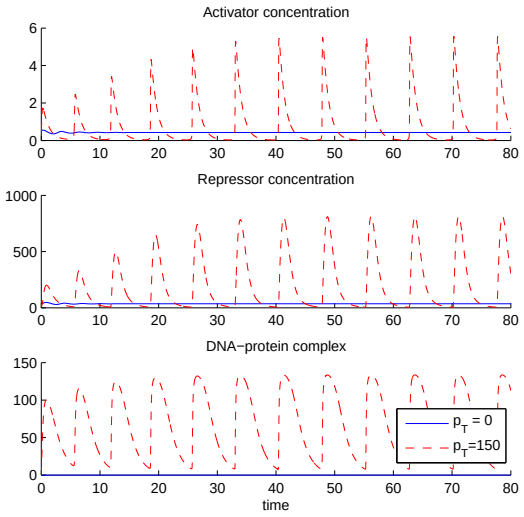


Fig. 4. These figures illustrate an activator-repressor that oscillates after addition of DNA binding sites $p$ to a non-oscillating activator-repressor. The originally stable system when isolated ($p_T = 0$) presents a periodic solution with addition of DNA binding sites ($p_T = 150$). System (10) was simulated with parameters $n = 2$, $\delta_A = 1$, $k_{on} = 10$, $k_{off} = 1000$, $\gamma_1 = \gamma_2 = \gamma_3 = .1$, $K_1 = K_2 = 300$, $K_{A0} = 0.04$, $K_{B0} = 0.004$ and $\delta_R = 1.5$.

This result is illustrated in Figure 3. The parameters of the system were chosen to satisfy conditions *(i)* and *(ii)* and the uniqueness of the equilibrium. Notice how the addition of binding sites removes the oscillation from the system.

### B. Repressor Binding Sites

Now we consider the system shown in Figure 1(c). The dynamics of the chemical equation (4) is incorporated in the isolated model (1) resulting in the model

$$\begin{aligned}\dot{A} &= -\delta_A A + f_1(A, R)\\ \dot{R} &= -\delta_R R + f_2(A) + k_{u2} C_2 - k_{b2} R(p_T - C_2)\\ \dot{C}_2 &= -k_{u2} C_2 + k_{b2} R(p_T - C_2).\end{aligned} \tag{10}$$

Note that, as before, the number and location of the equilibria of system (10) is the same as that of system (1).

Similarly to what was done in Section III-A, we employ a singular perturbation argument to reduce the order of the system. Define the small parameter $\epsilon := \delta_R / k_{u2}$ and let $k_{d2} := k_{u1}/k_{b1}$ be the dissociation constant. Define also the variable $Y_2 := R + C_2$. System (10) can be rewritten in the standard singular perturbation form as

$$\begin{aligned}\dot{A} &= -\delta_A A + f_1(A, Y_2 - C_2)\\ \dot{Y}_2 &= -\delta_R(Y_2 - C_2) + f_2(A)\\ \epsilon \dot{C}_2 &= -\delta_R C_2 + \frac{\delta_R}{k_{d2}}(Y_2 - C_2)(p_T - C_2).\end{aligned} \tag{11}$$

The slow manifold $C_2 = \psi(Y_2)$, obtained when setting $\epsilon = 0$ in system (11), is similar to the one obtained by solving (6). This manifold can also be shown to be attractive. The reduced system is thus given by

$$\begin{aligned} \dot{A} &= -\delta_A A + f_1(A, R) \\ \dot{R} &= \mathcal{S}_R(R, p_T)(-\delta_R R + f_2(A)), \end{aligned} \tag{12}$$

in which

$$\mathcal{S}_R(R, p_T) = 1 - \frac{\partial \psi(Y_2)}{\partial Y_2} = \frac{1}{1 + k_{d2} p_T (k_{d2} + R)^{-2}}.$$

Since $\mathcal{S}_R(R, p_T) \neq 0$, the equilibrium point $(A^*, R^*)$ of system (12) is the same as that of system (1). The Jacobian of this system, calculated at the equilibrium, as a function of $p_T$ is given by

$$J_R(p_T) = \begin{bmatrix} -\delta_a + \frac{\partial f_1(A^*, R^*)}{\partial A} & \frac{\partial f_1(A^*, R^*)}{\partial R} \\ \mathcal{S}_R^* \frac{\partial f_2(A^*)}{\partial A} & -\mathcal{S}_R^* \delta_R \end{bmatrix}, \tag{13}$$

in which we use the shorthand notation $\mathcal{S}_R^* := \mathcal{S}_R(R^*, p_T)$. Note that $0 < \mathcal{S}_R^* < 1$ is a strictly monotonically decreasing function of the parameter $p_T$. Note also that

$$\mathcal{S}_R^*|_{p_T=0} = 1 \text{ and } \lim_{p_T \to \infty} \mathcal{S}_R^* = 0. \tag{14}$$

The following lemma shows that an activator-repressor system with a stable equilibrium point can present periodic orbits upon addition of sufficient DNA binding sites with affinity to the repressor.

*Lemma 4:* Consider system (12) and let conditions *(i)* and *(ii)'* be satisfied. There exists $p^* > 0$ such that the solution of (12) is asymptotically stable if and only if $p_T < p^*$ and presents a periodic solution if $p_T > p^*$.

*Proof:* We first show that $\det(J_R(p_T)) > 0$ for all $p_T$. This follows from the fact that $\det(J_R(p_T)) = \mathcal{S}_R^* \det(J_0) > 0$, from condition *(i)*. Now we focus on

$$\operatorname{trace}(J_R(q_T)) = -\delta_a + \frac{\partial f_1(A^*, R^*)}{\partial A} - \mathcal{S}_R^* \delta_R.$$

From (14) and condition $(ii)'$, when $p_T = 0$ $\operatorname{trace}(J_R(0)) < 0$. Additionally, as

$$\text{as } p_T \to \infty,\ \operatorname{trace}(J_R(p_T)) \to -\delta_a + \frac{\partial}{\partial A} f_1(A^*, R*) > 0.$$

Since the trace is a monotonic smooth function of $p_T$, one can apply the intermediate value theorem to show that there is an unique $0 < p^* < \infty$ such that $\operatorname{trace}(J_R(p^*)) = 0$. Since $\det(J_R(p^*)) > 0$, the eigenvalues of $J_R(p^*)$ are imaginary. From the monotonicity of the trace with respect to $p_T$, it follows that the real part of the eigenvalues of $J_A(q_T)$ is negative for all $0 \leq p_T < p^*$ and positive for all $q_T > q^*$. It follows that the system goes through a Hopf bifurcation at $p_T = p^*$, and thus presents a periodic solution for $p_T > p^*$, while it converges to the equilibrium for $0 \leq p_T < p^*$. ■

This result is illustrated in Figure 4. The parameters of the system were chosen to satisfy conditions *(i)* and *(ii)'*. Notice how the addition of binding sites with affinity to the repressor induces oscillations in a non-oscillating system .

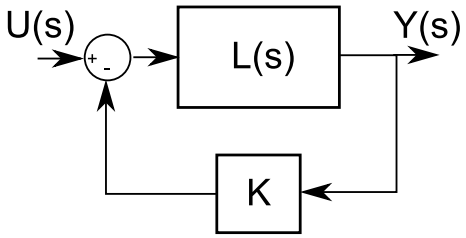


Fig. 5. A simple feedback system with an open loop transfer function $L(s)$ and the feedback gain $K$.

## IV. Root Locus Interpretation

Consider the feedback system in Figure 5 with a feedback gain $K$ and open loop transfer function $L(s) = N(s)/D(s)$. The poles of the closed loop system are given by the roots of the equation $\Delta(s) = D(s) + KN(s) = 0$ and can be graphically depicted as a function of $K$ using the root locus diagram. This idea can be employed to find the eigenvalues of the Jacobians (8) and (13) as a function of $\mathcal{S}_A^*$ and $SR$ respectively.

Consider, for example, system (7). The eigenvalues of its Jacobian (8) are given by the roots of the characteristic equation

$$\begin{aligned} \Delta_A(\lambda) &= \lambda^2 - (\mathcal{S}_A^* a + d)\lambda + \mathcal{S}_A^*(ad - bc) \\ &= \lambda^2 - d\lambda + \mathcal{S}_A^*(-a\lambda + ad - bc), \end{aligned}$$

in which $a = -\delta_A + \frac{\partial f_1(A^*, R^*)}{\partial A}$, $b = \frac{\partial f_1(A^*, R^*)}{\partial R}$, $c = \frac{\partial f_2(A^*)}{\partial A}$ and $d = -\delta_R$. The eigenvalues are therefore identical to the location of the poles of the closed loop system of Figure 5 with gain $K = \mathcal{S}_A^*$ and open loop transfer function given by

$$L(s) = -\frac{as - (ad - bc)}{s^2 - ds}. \tag{15}$$

This transfer function has one zero at $s = (ad - bc)/a > 0$ (conditions *(i)* and *(ii)*) and poles at $s = 0$ and $s = d < 0$. The root locus diagram is, therefore, of the form shown in Figure 6(a). Since the "gain" $\mathcal{S}_A^*$ is such that $0 < \mathcal{S}_A^* \leq 1$, the actual loci of the eigenvalues of the Jacobian are restricted to the red line. Arrow heads indicate the movement of the eigenvalues as $q_T$ increases. The figure also highlights the point $q_T = q^*$ at which the system undergoes a Hopf bifurcation, and it shows how the signal of the real parts of the eigenvalues goes from positive to negative as $q_T$ increases.

This idea can also be applied to system (12). In this case, the eigenvalues of Jacobian (13) are the roots of the characteristic equation

$$\Delta_R(\lambda) = \lambda^2 - a\lambda + \mathcal{S}_{eq}(p_T)(-d\lambda + ad - bc),$$

in which $a$, $b$, $c$ and $d$ are the same as defined above. Here, it is assumed that the feedback gain is $K_R = \mathcal{S}_R^*$ and the open loop transfer function given by

$$L(s) = -\frac{ds - (ad - bc)}{s^2 - as}. \tag{16}$$

(a) Addition of Binding Sites to Activator

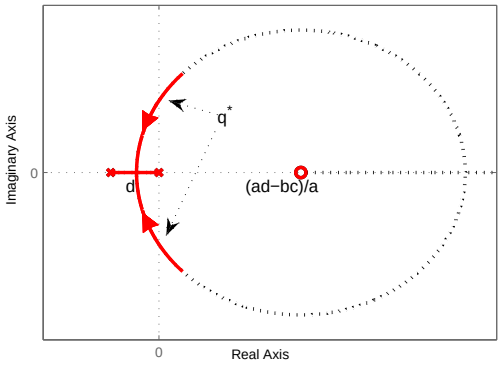


(b) Addition of Binding Sites to Repressor

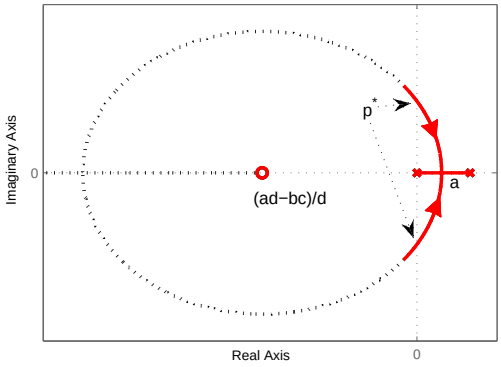


Fig. 6. In plots (a) and (b), the dashed lines indicate the root locus diagram of the closed loop systems obtained from the open loop transfer functions (15) and (16) respectively. The red lines in plots (a) and (b) indicate the possible values for the eigenvalues of Jacobians (8) and (13) respectively, and the arrows indicate the movement of the eigenvalue as the quantity of binding sites increases. Points $q^*$ and $p^*$ at which systems (5) and (10) go through a Hopf bifurcation are also indicated.

This transfer function now has a zero at $s = (ad-bc)/d < 0$ (condition *(i)*) and poles at $s = 0$ and $s = a > 0$ (condition *(ii)'*). The root locus diagram is, therefore, of the form shown in Figure 6(b). Again, due to the bounds $0 < \mathcal{S}_R^* \leq 1$, the eigenvalues of the Jacobian are restricted to the red line. The arrows indicate the movement of the eigenvalues as $p_T$ increases. The point at $p_T = p^*$ in which the system undergoes a Hopf bifurcation is annotated.

Figure 6 also gives a graphical interpretation to conditions *(ii)* and *(ii)'*. These conditions guarantee that, in both cases, the zero and the non-null pole of the transfer functions have opposite signs. This ensures that the root locus diagram crosses the imaginary axis at $s \neq 0$, a necessary condition for a Hopf bifurcation to occur.

## V. Conclusion

In this paper, we presented a method to tune a two-dimensional model of an activator-repressor oscillator by addition of binding sites with affinity to either the activator or repressor proteins. This method exploits the retroactivity effect to alter the timescale difference between the two protein dynamics, a key parameter in determining the oscillation of this system. As a result, we have shown that the concentration of additional binding sites to the system becomes a bifurcation parameter.

These results provide a tool for altering the behavior of an activator-repressor motif by the addition of extra DNA binding sites. This method for tuning the clock is experimentally simple when compared to standard tuning methods involving changes to promoter sites and protein degradation tags, since it can be realized by simple transformation or transfection of DNA containing the specific sequence. More generally, we have shown how to employ retroactivity to adjust the effective timescales of individual processes in Synthetic Biology.These results also suggest that retroactivity has potential to be a mechanism by which relative timescales are adjusted in natural systems in order to obtain a specific behavior.

We are currently expanding the results of this paper by analyzing the effect of adding DNA binding sites with affinity to the activator and the repressor simultaneously. We are further studying the potential of tuning the frequency of the activator-repressor clock by changing the amount and affinity of the DNA sites. Finally, we are also considering the effect of incorporating the mRNA dynamics in this system, as this has potential for a richer dynamic behavior.

## References


[1] J. R. Pomerening, E. D. Sontag, and J. E. Ferrell, "Building a cell cycle oscillator: hysteresis and bistability in the activation of cdc2," *Nature Cell Biology*, vol. 5, pp. 346–351, 2003.

[2] J. Dunlap, "The molecular bases for circadian clocks," *Cell*, vol. 96, pp. 271–290, 1999.

[3] T. Danino, O. Mondragn-Palomino, L. Tsimring, and J. Hasty, "A synchronized quorum of genetic clocks," *Nature*, vol. 463, pp. 326–330, 2009.

[4] M. B. Elowitz and S. Leibler, "A synthetic oscillatory network of transcriptional regulators," *Nature*, vol. 403, pp. 339–342, 2000.

[5] M. Tigges, T. T. Marquez-Lago, J. Stelling, and M. Fussenegger, "A tunable synthetic mammalian oscillator," *Nature*, vol. 457, pp. 309–312, 2009.

[6] M. R. Atkinson, M. A. Savageau, J. T. Meyers, and A. J. Ninfa, "Development of genetic circuitry exhibiting toggle switch or oscillatory behavior in *escherichia coli*," *Cell*, vol. 113, pp. 597–607, 2003.

[7] J. Stricker, S. Cookson, M. R. Bennett, W. H. Mather, L. S. Tsimring, and J. Hasty, "A fast, robust and tunable synthetic gene oscillator," *Nature*, vol. 456, pp. 516–519, 2008.

[8] D. Del Vecchio, "Design of an activator-repressor clock in *e. coli*," in *Proc. American Control Conference*, 2007.

[9] E. Andrianantoandro, S. Basu, D. K. Karig, and R. Weiss, "Synthetic biology: New engineering rules for an emerging discipline," *Molecular Systems Biology*, pp. 1–14, 2006.

[10] J. M. Flynn, I. Levchenko, M. Seidel, S. H. Wickner, R. T. Sauer, and T. A. Baker, "Overlapping recognition determinants within the ssra degradation tag allow modulation of proteolysis," *PNAS*, vol. 98, no. 19, 2001.

[11] D. Del Vecchio, A. J. Ninfa, and E. D. Sontag, "Modular cell biology: Retroactivity and insulation," *Nature/EMBO Molecular Systems Biology*, vol. 4:161, 2008.

[12] S. Jayanthi and D. Del Vecchio, "On the compromise between retroactivity attenuation and noise amplification in gene regulatory networks," in *Proc. Conference on Decision and Control*, dec. 2009.

[13] J. Sambrook and D. W. Russel, *Molecular Cloning: a laboratory Manual*, 3rd ed. Cold Spring Harbor, 2001.

[14] U. Alon, *An introduction to systems biology. Design principles of biological circuits*. Chapman-Hall, 2007.

[15] H. Khalil, *Nonlinear Systems*. Prentice Hall, 2002.